Technical Note

An Arthroscopy-Assisted Mini-Invasive Technique to Create a Chronic Rabbit Model With Massive and Retracted Supraspinatus Rotator Cuff Tears

Junjie Xu, M.D., Kang Han, M.D., Wei Su, M.D., and Jinzhong Zhao, M.D.

Abstract: Understanding the pathophysiology of rotator cuff tears (RCTs) in animal models is of great importance, as it helps in the development of repair strategies and therapeutic treatments for rotator cuff diseases in humans. This Technical Note describes a comprehensive step-by-step description of an arthroscopic-assisted minimally invasive RCT model in rabbits. This technique is beneficial because the rabbit has rotator cuffs anatomically similar to those of humans, and it has been widely used as a preclinical animal model in the basic science literature. Compared with other small animals (e.g., mice and rats), the advantage of the rabbit model is that it can test the effectiveness and healing process of new surgical repair techniques that require relatively larger anatomical structures. Moreover, it is more cost-effective compared with larger animal models, such as sheep and canines. This arthroscopic-assisted mini-invasive technique to create an RCT model may have a better effect on simulating the degenerative and chronic RCT state in humans than the commonly used open surgery, along with an earlier return to activities, less scarring and tissue adhesion, fewer injuries to the deltoid, and fewer complications.

Rotator cuff tears (RCTs) are a common pathologic condition that frequently cause persistent pain and functional impairments in the affected shoulder joint in humans.[1-4] Preclinical animal models, as effective and rich tools in research, help clinicians further understand the basics of human pathologies and reparative processes, especially at the cellular and tissue levels, as well as for the evaluation of new therapeutics and surgical techniques.[5-9] Numerous basic studies have used rabbit models to investigate rotator cuff diseases and healing capacities after rotator cuff repair.[10-16] The rabbit model of RCT is important because it is a reasonable and reliable animal model, and findings from such studies may accurately reflect the chronic and degenerative status of RCTs in humans. However, in these studies, rotator cuff repairs were performed using an acute tear model or a chronic tear model created by an open surgery. These disease models inevitably result in some interference factors, such as undue acute inflammatory responses and excessive tissue adhesion caused by additional open surgery. These factors affect assessments in animal models and further extrapolations to clinical scenarios.

Therefore, the purpose of this Technical Note is to describe our arthroscopic-assisted mini-invasive procedure to create a chronic, massive, and retracted RCT model in rabbits. This technique is reproducible and simple for arthroscopic surgeons and can be applied to create preclinical RCTs models to evaluate rotator cuff diseases and repair surgeries, both histologically and biomechanically.

Surgical Technique

The use of laboratory animals was approved by the institutional animal care and use committee. The step-by-step procedure is presented in Table 1.

From the Department of Sports Medicine, Shanghai Jiao Tong University Affiliated Sixth People's Hospital, Shanghai, China.

Drs. Su and Zhao contributed to the specific design of the detailed procedure.

The authors report the following potential conflicts of interest or sources of funding: funding from the Youth Program of National Natural Science Foundation of China, 82002274, and Shanghai Rising-Star Program, 21QC1401300. Full ICMJE author disclosure forms are available for this article online, as supplementary material.

Junjie Xu and Kang Han contributed equally to this article.

Received December 22, 2021; accepted February 4, 2022.

Address correspondence to Jinzhong Zhao, Department of Sports Medicine, Shanghai Jiao Tong University Affiliated Sixth People's Hospital, 600 Yishan Rd., Shanghai, China. E-mail: jzzhao@sjtu.edu.cn

2212-6287/211816

https://doi.org/10.1016/j.eats.2022.02.001

Table 1. Step-by-Step Procedure

1. Anesthetize and position the rabbit.
2. Palpate the surface marks and create three mini-incisions for portals.
3. Elevate the subdeltoid space, identify and mark the borders of the supraspinatus (SSP) tendon.
4. Detach and release the distal half of the SSP tendon portion and retrieve it from the middle-lateral portal.
5. Confirm the massive and retracted SPP tears arthroscopically.
6. Close the mini-incisions.
7. Postoperative rehabilitation and waiting for a chronic status

Step 1: Anesthetization and Position

One skeletally mature New Zealand White rabbit (male, 3.4 kg) is anesthetized using pentobarbital (3%, 30 mg/kg) through intravenous injection and the incision site of the shoulder is then injected with lidocaine subcutaneously. We place 2 wet gauzes on the rabbit' eyes to prevent corneal trauma and drying. Then, the rabbit is positioned supine on an incandescent lamp heating pad. We fix the nonsurgical limbs (1 forelimb and 2 hindlimbs) on the surgical bed using bandages to prevent the movement of the rabbit during the procedure. The surgical limb can move freely. Next, the hair of the surgical forelimb is shaved and the skin is disinfected with iodophor 3 times. The rabbit is covered with a sterile surgical drape, with a small window made to access the surgical site (Fig 1A). After externally rotating the shoulder, the greater tuberosity (GT) is palpated and the supraspinatus (SSP) tendon insertion region between the clavicle and scapular spine is roughly identified through pressing the upper part of the GT (Fig 1B). The SSP insertion region is appropriately 10 mm long.

Step 2: Mini-Incision and Portal Creation

The middle lateral (M-L), anterolateral (A-L), and posterolateral portals (P-L) were marked for visualization (Fig 1B). Then, a longitudinal middle mini-incision (~6-8 mm) was created using a #15-blade scalpel at the SSP insertion region in the direction of the distal clavicle to the deltoid tuberosity, along with anterolateral and posterolateral mini-incisions (~3-4 mm) for portals (Fig 1C).

Subcutaneous flaps were mobilized, and the deltoid was tensioned and subsequently punctured using a blade when the forelimb was adducted, extended, and externally rotated. The subdeltoid space was then bluntly separated using a needle holder. In this rabbit model, as the routine arthroscope for humans is too large, we used an otoscope with a battery-powered illuminant (Jiu Tan, Shenzhen, China) as an "arthroscope" for monitoring (Fig 2A). Two mini-tissue probes (diameter = 1 mm) penetrated the skin and subcutaneous tissues into the subdeltoid space through the A-L and P-L portals, respectively. After lifting the 2 probes to enlarge the subdeltoid space, a 2.7-mm "arthroscope" was positioned in the previously established middle mini-incision, which served as the M-L viewing portal (Fig 2B).

Step 3: SSP Identification and Separation

Under monitoring, the SSP tendon could be fully identified when externally or internally rotating the shoulder. In the rabbit model, the SSP tendon, a shiny, white, and thick structure, was attached to nearly the entire upper part of the humeral head, which was approximately 1 cm in width (Fig 3A, Video 1). After confirming the SSP anterior and posterior borders (Fig 3 B and 3C) and debriding the surrounding tissues in intervals, two 2-0 sutures (Ethicon, Piscataway, NJ) were introduced into the A-L and P-L portals, respectively, to mark the distal SSP margins at its anterior and posterior insertion under monitoring through the M-L portal (Fig 4 A-C, Video 1). Extending and adducting the forelimb helps to maintain SSP tension, which

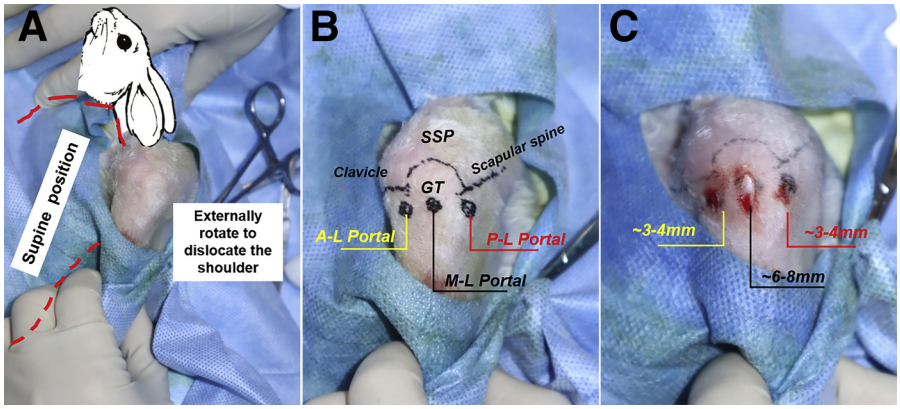

Fig 1. (A) The animal is in a supine position, with left shoulder external rotation. (B) The surface markings are shown on the left shoulder, including the clavicle, scapular spine, greater tuberosity (GT), which helps in identifying the arthroscopic posterolateral (P-L), anteroposterior (A-L), and middle lateral (M-L) portals shown on the shoulder. The entire insertion of the supraspinatus (SSP) tendon could be palpated on the upper portion of the GT. (C) Three mini-incisions for arthroscopic portals (~3-4 mm for P-L and A-L portals; ~6-8 mm for M-L portal) were created for visualization and inspection, with the insertion of instruments under vision for working.

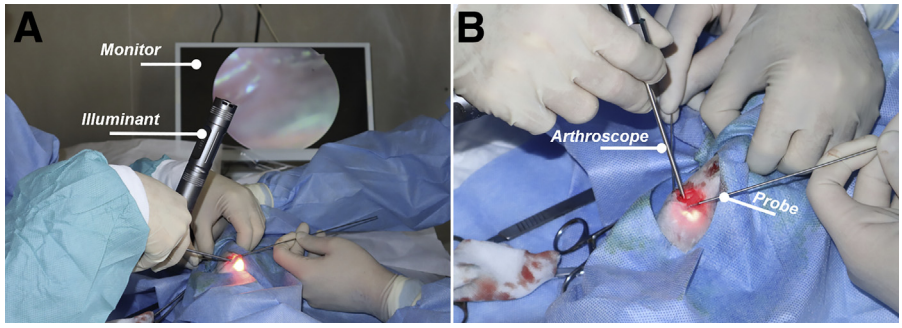

Fig 2. (A) An otoscope with a battery-powered illuminant is used as an "arthroscope" for monitoring. (B) Two mini tissue probes are inserted into the subdeltoid space through the lateral-posterior and anteroposterior portals and then lifted to enlarge a sufficient space for monitoring by "arthroscope" through the middle-posterior portal.

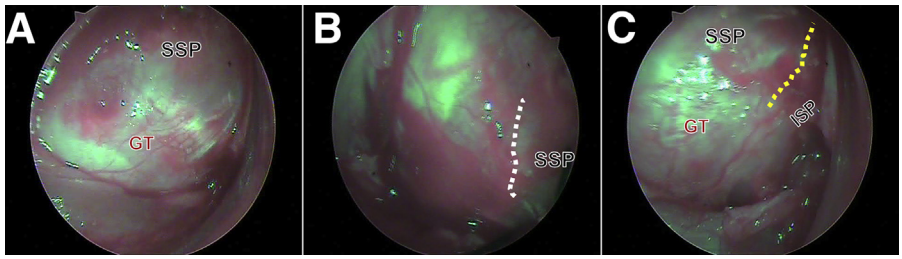

Fig 3. (A) After lifting 2 probes to form a sufficiently big subdeltoid space, the supraspinatus (SSP) tendon could be brought into the arthroscopic view when the forelimb was rotated. The SSP insertion site covers almost the entire upper portion of the greater tuberosity (GT). (B) The anterior border of the SSP (while dotted line) is identified in the superior and anterior edge of the GT under the anterolateral arthroscopic view. (C) The posterior border of the SSP (yellow dotted line) is identified in the superior and posterior edge of the GT under the posterior-lateral arthroscopic view, which is the interval between SSP and the infraspinatus tendon.

allows the suture to easily penetrate the tendon. Thereafter, both outer suture ends were retrieved from the M-L portal after introducing them into their respective portals.

Using these the suture as marker, we delivered the anterior or posterior border of the SSP to the M-L portal when rotating the shoulder so that we can visualize it through portal, respectively. Then, we created an anterior or posterior mini-incision at the interval near the border of the SSP, respectively, using the tip part of a #15-blade scalpel through this portal. A 2-mm K-wire was introduced into the A-L portal to enter the plane between the SSP tendon and the articular surface of the humeral head from the anterior border (Fig 5A) to the posterior bolder (Fig 5B) of the SSP and then retrieved from the P-L portal. Next, this K-wire manually slid from the distal SSP insertion site to the proximal region, releasing the distal SSP tendon portion from the adjacent rotator cuffs (Fig 5C). Giving traction to the 2 sutures helps to release the interval of this plane to allow the K-wire to easily slide along the plane under the SSP tendon.

Subsequently, the SSP tendon was carefully detached from the humeral head from the anterior insertion to

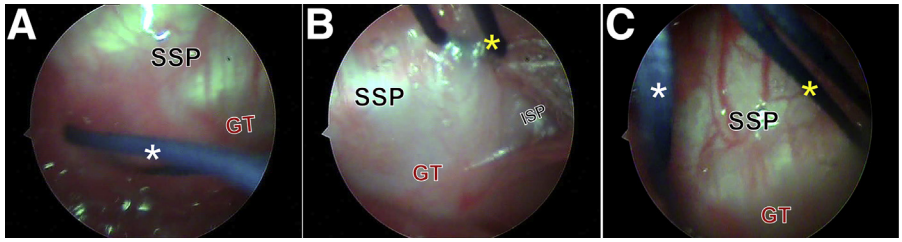

Fig 4. (A) A 2-0 suture (white asterisk) is shuttled through the anterolateral portal to mark the anterior and distal insertion site of the supraspinatus (SSP) tendon in the middle-lateral view. (B) Similarly, another suture (yellow asterisk) is used to mark the posterior and distal insertion site through the posterolateral portal. (C) Both the ends of these 2 marking sutures are retrieved from the M-L portal. (GT, greater tuberosity; ISP, infraspinatus tendon; M-L, middle lateral.).

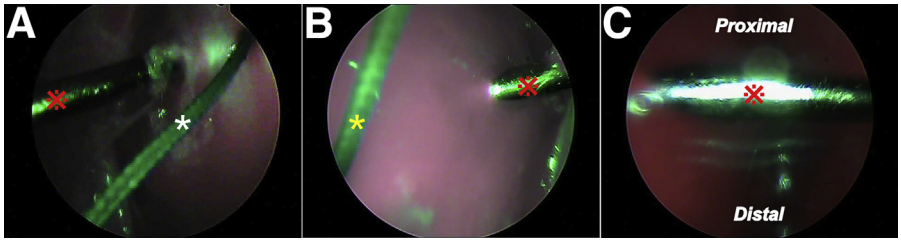

Fig 5. (A) A 2-mm K-wire (cross asterisk) enters the plane between the supraspinatus (SSP) tendon and the articular surface of the humeral head from the rotator cuff interval to (B) the interval between supraspinatus and infraspinatus tendons. (C) After retrieving the K-wire from the posterolateral portal, the distal portion of the SSP tendon is released from the adjacent rotator cuffs by manually sliding the K-wire from the distal to the proximal. White and yellow asterisks denote anterior and posterior sutures, respectively.

Fig 6. (A) An #15-blade scalpel (red triangle) is introduced into the medial lateral portal to cut the anterior portion and (B) the posterior insertion of the supraspinatus (SSP) tendon. (C) Then the entire SSP tendon is detached from the greater tuberosity (GT), with its stump slightly retracted. White and yellow asterisks denote anterior and posterior sutures, respectively.

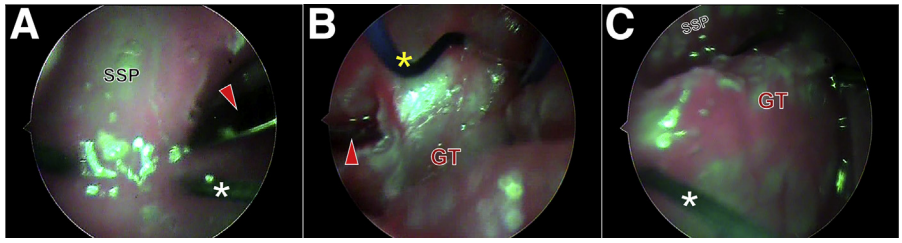

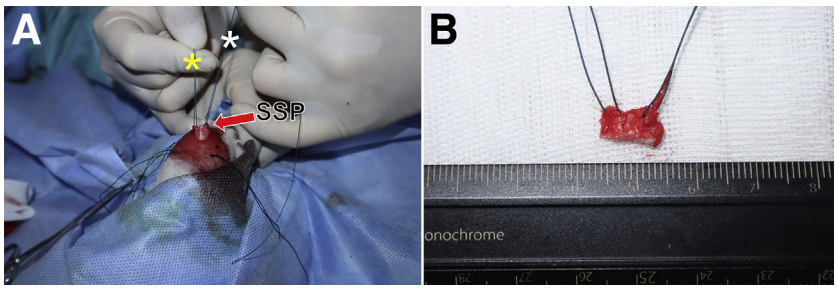

Fig 7. (A) The detached supraspinatus (SSP) tendon is pulled out from the middle lateral portal using 2 marking sutures (white and yellow asterisks). (B) The distal half portion of the SSP tendon is cut to create full-thickness massive defects.

the posterior using a #15-blade scalpel through the M-L portal under monitoring in the A-L (Fig 6A, Video 1) or P-L (Fig 6B, Video 1) viewing portals, respectively. The SPP footprint on the GT was fully exposed and the distal SSP tendon was slightly retracted (Fig 6C, Video 1).

Step 4: Full-Thickness SSP Defects Creation Through Middle-Lateral Mini-Incision

The entire detached SSP tendon was pulled out from the longitudinal mini-incision (Fig 7A), and the distal half of the tendon portion was cut using a #15-blade

Fig 8. (A) In the anterolateral view, the supraspinatus (SSP) tendon stump humeral head (HH) and the intra-articular biceps (B) are exposed. (B) No tendon tissue remains on the footprint, and the massive full-thickness SSP defects are confirmed by arthroscope through the middle lateral portal. (C) A microtweezer is used to check the retraction of the SSP tendon stump, which could not be pulled back fully onto its native footprint.

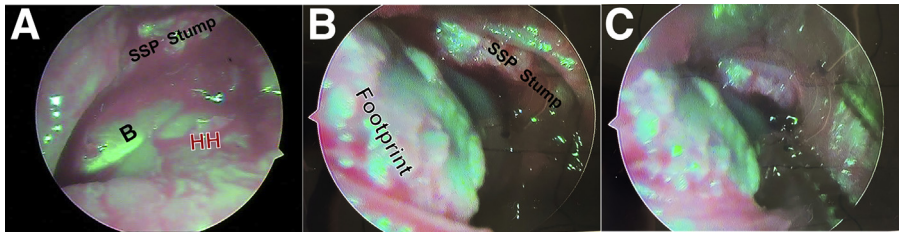

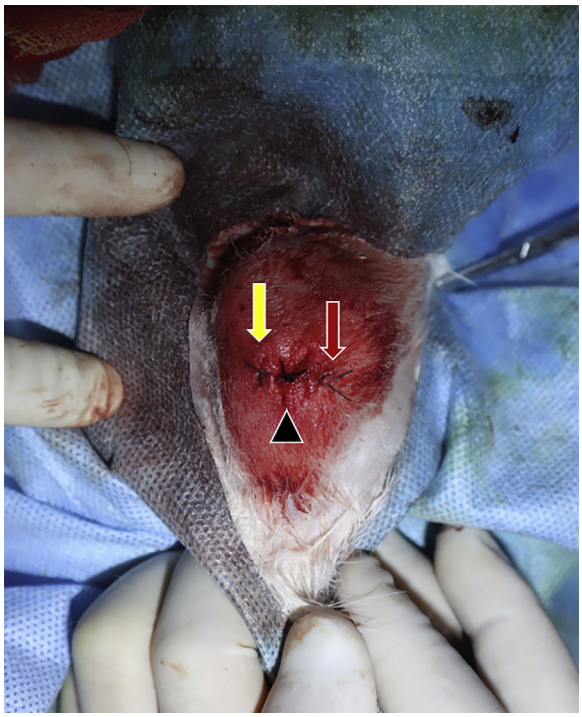

Fig 9. The anterolateral (yellow arrow) and posterolateral (red arrow) incisions are closed using 4-0 sutures while closing the middle-lateral incision (black triangle) using a 3-0 suture.

scalpel to create massive and full-thickness SSP defects (~10 mm long and ~3-4 mm wide) (Fig 7B). The SSP tendon was then released and retracted back into the mini-incision.

Step 5: Arthroscopic Confirmation

Under monitoring through the M-L viewing portal, the defective SSP tendon was confirmed to retract back into the subacromial space and the humeral head was exposed (Fig 8A, Video 1). This indicates stage-2 retraction of the SSP according to Patte's classification.[17] We also checked that there were no remaining SSP tendon tissues on the footprint (Fig 8B). We used an ophthalmic micro-tweezer to confirm that the SSP tendon could not be pulled back on the footprint. Therefore, this massive and retracted SSP defects were created.

Fig 10. The specialized instruments for this arthroscopy-assistant animal model creation, including an otoscopic system that comprises 2.7-mm otoscope, camera and illuminant, #15-blade, and bending or straight micro-tweezer.

Table 2. Tips and Tricks

1. Sufficient enlargements of subdeltoid space by lifting the tissue probes are critical to fully expose the supraspinatus (SSP) tendon and its insertion on the greater tuberosity in the arthroscopic view.
2. Additional skin traction strings at appropriate places help to elevate the subdeltoid space.
3. Careful separation of the subdeltoid space and cautious stitching of the SSP tendon using sutures help in avoiding microvascular damage to the surface of the greater tuberosity and the SSP, which is critical for maintaining effective arthroscopic visualization in the absence of the irrigation system and trocar instruments.
4. Effective release of the distal part of the SSP helps to retrieve the tendon from the middle-lateral portal.
5. Opportunely tensioning the marking sutures at the anterior or posterior border opportunely is important to cut the resilient SSP tendon tissues.
6. A relatively larger mid-lateral incision helps to retrieve the SSP tendon successfully.

Step 6: Mini-Incision and Portal Closure

The middle incision is closed using the 3-0 sutures (Ethicon) and the anterior or posterior portal using 4-0 sutures (Ethicon) (Fig 9). The total procedure time of this RCT model from start to finish was approximately 15 minutes. The specialized instruments used for generating the animal model are shown in Fig 10. The tips and tricks are listed in Table 2.

Step 7: Postoperative Care

Postoperatively, this animal was allowed to recover from anesthesia in a recovery cage with a heating incandescent lamp. A prophylactic antibiotic—ampicillin 50 mg/kg body weight—was administered for 5 days after surgery. Postoperatively, the animals were returned to the housing cage, cared for by a veterinarian, and monitored daily for signs of pain and infection. Based on the findings in rabbits reported by Abdou et al.,[10] 4 weeks is the suggested waiting period

Table 3. Advantages and Disadvantages

Advantages
1. Minimally invasive
2. Less risk of injury to the deltoid and other adjacent anatomical structures
3. Less risk of scarring and undue tissue adhesion
4. Less risk of the early acute inflammatory tissue reactions as a result of tendon tears

Disadvantages
1. Requirement of instruments for animal models
2. Requirement of relatively high surgical skills and technically demanding
3. Relatively more time-consuming to create defective models with arthroscopy

for making a chronic repairable RCT animal model for human research.

Discussion

Some animal RCTs models, acute or chronic, described in canines, rabbits, rats, and mice, have been widely used in many studies on rotator cuff disease.[5,6,18,19] The rabbit is a relatively cost-effective model with a larger anatomical structure than rodents, which increases the reproducibility and operability of the defect model creation and repair surgery and eases the difficulties associated with histologic and biomechanical testing. Meanwhile, it shortens research periods when compared with the larger animals including the sheep and canine models. The RCT model is essential for further understanding the pathophysiology of rotator cuff diseases in humans, such as degenerative tendon pathologies and fatty infiltration of the muscles, and the healing effects of therapeutic treatments using drugs and surgeries.[10,12,13,15,16]

In this Technical Note, we successfully created a massive and retracted RCT model in rabbits using an arthroscopy-assisted minimally invasive approach. According to Abdou et al.,[10] 4 weeks is the suggested waiting period to make a chronic RCT rabbit model for human research. In recent rabbit studies on rotator cuff diseases, the chronic RCT model has been highlighted and described in detail to simulate the chronic inflammatory status with degenerative tissues in humans as much as possible.[6,11,14] However, the open surgery for generating chronic RCT model, especially for massive tears, inevitably results in additional injuries of adjacent anatomical structures when establishing both a longer surgical incision and a larger surgical approach.[20,21] In this context, the undue acute inflammatory responses, local tissue infections, subsequent excessive tissue adhesion, long-term postoperative pain, and shoulder movement disorder can be caused by open surgery.[22] These posttraumatic tissue responses may substantially influence the effective translation of animal models to clinical conditions, as most RCTs in humans are age-related and degenerative, rather than severe and trauma-induced.[1-3] In contrast, the arthroscopy-assisted approach for creating RCTs is minimally invasive. In the technique described here, only mini-incisions were used to create lateral portals for working and viewing when performing all procedures. This technique has many advantages (Table 3), although it is technically demanding. As arthroscopy is becoming the standard of care for most human shoulder pathologies, more favorable factors, such as its minimally invasive nature, a shorter period of postoperative pain, less scarring and injury to the deltoid, fewer complications, and an early return to routine activities, can be found using this arthroscopy-assisted rabbit RCT model. In addition to animal welfare, these advantages may renew the surgical armamentarium for animal studies and provide a strategy to create a rotator cuff disease model, as most clinicians expect more accurate and effective models to simulate the clinical disease state as much as possible.

Acknowledgments

The authors thank Dr. Wu for providing guidelines and help with video editing and postproduction.

References

1. Sommer MC, Wagner E, Zhu S, et al. Complications of superior capsule reconstruction for the treatment of functionally irreparable rotator cuff tears: A systematic review. *Arthroscopy* 2021;37:2960-2972. https://doi.org/10.1016/j.arthro.2021.03.076.
2. Reddy AK, Shepard S, Ottwell R, et al. Over 30% of systematic reviews and meta-analyses focused on rotator cuff tear treatments contained spin in the abstract. *Arthroscopy* 2021;37:2953-2959. https://doi.org/10.1016/j.arthro.2021.03.066.
3. Sheean AJ, Hartzler RU, Burkhart SS. Arthroscopic rotator cuff repair in 2019: Linked, double row repair for achieving higher healing rates and optimal clinical outcomes. *Arthroscopy* 2019;35:2749-2755. https://doi.org/10.1016/j.arthro.2019.02.048.
4. Ryan J, Imbergamo C, Sudah S, et al. Platelet-rich product supplementation in rotator cuff repair reduces retear rates and improves clinical outcomes: A meta-analysis of randomized controlled trials. *Arthroscopy* 2021;37:2608-2624. https://doi.org/10.1016/j.arthro.2021.03.010.
5. Miller M, Kazmers NH, Chalmers PN, Tashjian RZ, Jurynec MJ. Supraspinatus rotator cuff repair: A mouse model and technique. *Arthrosc Tech* 2021;10:e1949-e1954. https://doi.org/10.1016/j.eats.2021.04.023.
6. Xu J, Su W, Chen J, et al. The effect of antiosteoporosis therapy with risedronate on rotator cuff healing in an osteoporotic rat model. *Am J Sports Med* 2021;49:2074-2084. https://doi.org/10.1177/03635465211011748.
7. Rhee S-M, Youn S-M, Ko YW, Kwon TY, Park Y-K, Rhee YG. retracted rotator cuff repairs heal with disorganized fibrogenesis without affecting biomechanical properties: A comparative animal model study. *Arthroscopy* 2021;37:3423-3431. https://doi.org/10.1016/j.arthro.2021.06.025.
8. Rhee S-M, Kim YH, Park JH, et al. Allogenic dermal fibroblasts improve tendon-to-bone healing in a rabbit model of chronic rotator cuff tear compared to platelet-rich plasma [published online December 27, 2021]. Arthroscopy, https://dx.doi.org/10.1016/j.arthro.2021.12.029.
9. Xu J, Li Y, Zhang X, et al. The biomechanical and histological processes of rerouting biceps to treat chronic irreparable rotator cuff tears in a rabbit model. *Am J Sports Med* 2022, 3635465211062914. https://doi.org/10.1177/03635465211062914.

10. Abdou MA, Kim G-E, Kim J, et al. How long should we wait to create the Goutallier stage 2 fatty infiltrations in the rabbit shoulder for repairable rotator cuff tear model? *Biomed Res Int* 2019;2019, 7387131. https://doi.org/10.1155/2019/7387131.
11. Xu J, Li Y, Ye Z, et al. Biceps augmentation outperforms tear completion repair or in situ repair for bursal-sided partial-thickness rotator cuff tears in a rabbit model. *Am J Sports Med* 2021, 3635465211053334. https://doi.org/10.1177/03635465211053334.
12. Su W, Qi W, Li X, Zhao S, Jiang J, Zhao J. Effect of suture absorbability on rotator cuff healing in a rabbit rotator cuff repair model. *Am J Sports Med* 2018;46:2743-2754. https://doi.org/10.1177/0363546518787181.
13. Su W, Li X, Zhao S, et al. Native enthesis preservation versus removal in rotator cuff repair in a rabbit model. *Arthroscopy* 2018;34:2054-2062. https://doi.org/10.1016/j.arthro.2018.03.005.
14. Li X, Shen P, Su W, Zhao S, Zhao J. Into-tunnel repair versus onto-surface repair for rotator cuff tears in a rabbit model. *Am J Sports Med* 2018;46:1711-1719. https://doi.org/10.1177/0363546518764685.
15. Su W, Wang Z, Jiang J, Liu X, Zhao J, Zhang Z. Promoting tendon to bone integration using graphene oxide-doped electrospun poly(lactic-co-glycolic acid) nanofibrous membrane. *Int J Nanomedicine* 2019;14:1835-1847. https://doi.org/10.2147/IJN.S183842.
16. Chung SW, Park H, Kwon J, Choe GY, Kim SH, Oh JH. Effect of hypercholesterolemia on fatty infiltration and quality of tendon-to-bone healing in a rabbit model of a chronic rotator cuff tear: Electrophysiological, biomechanical, and histological analyses. *Am J Sports Med* 2016;44:1153-1164. https://doi.org/10.1177/0363546515627816.
17. Patte D. Classification of rotator cuff lesions. *Clin Orthop Relat Res* 1990;(254):81-86.
18. Rodeo SA, Potter HG, Kawamura S, Turner AS, Kim HJ, Atkinson BL. Biologic augmentation of rotator cuff tendon-healing with use of a mixture of osteoinductive growth factors. *J Bone Joint Surg Am* 2007;89:2485-2497. https://doi.org/10.2106/JBJS.C.01627.
19. Chen H, Li S, Xiao H, et al. Effect of exercise intensity on the healing of the bone-tendon interface: A mouse rotator cuff injury model study. *Am J Sports Med* 2021;49:2064-2073. https://doi.org/10.1177/03635465211011751.
20. Yildiz F, Bilsel K, Pulatkan A, et al. Comparison of two different superior capsule reconstruction methods in the treatment of chronic irreparable rotator cuff tears: A biomechanical and histologic study in rabbit models. *J Shoulder Elbow Surg* 2019;28:530-538. https://doi.org/10.1016/j.jse.2018.08.022.
21. Hasegawa A, Mihata T, Itami Y, Fukunishi K, Neo M. Histologic changes during healing with autologous fascia lata graft after superior capsule reconstruction in rabbit model. *J Shoulder Elbow Surg* 2021;30:2247-2259. https://doi.org/10.1016/j.jse.2021.02.019.
22. Broek RPG ten, Bakkum EA, Laarhoven CJHM, van Goor H. Epidemiology and prevention of postsurgical adhesions revisited. *Ann Surg* 2016;263:12-19. https://doi.org/10.1097/SLA.0000000000001286.